Elsevier Editorial System(tm) for Carbohydrate Polymers

Manuscript Draft

Manuscript Number:

Title: Preparation of chitosan-hydroxyapatite composite mono-fiber using coagulation method and their mechanical properties

Article Type: Research Paper

Keywords: artificial ligament, fiber, chitosan, hydroxyapatite, coagulation method, mechanical property

Corresponding Author: Dr. Yuki Shirosaki, Ph. D.

Corresponding Author's Institution: Kyushu Institute of Technology

First Author: Takuma Okada

Order of Authors: Takuma Okada; Yuta Nobunaga; Toshiisa Konishi; Tomohiko Yoshioka; Satoshi Hayakawa; Maria A Lopes; Toshiki Miyazaki; Yuki Shirosaki, Ph. D.

Abstract: Autograft has been carried out for anterior cruciate ligament (ACL) reconstruction surgery. However, it has negative aspect because patients lose their healthy ligaments from other part. Sometimes, artificial ligament from synthetic polymer such as PET is used, however it does not have bone-bonding ability and stays long time in body. We focus on a chitosan-hydroxyapatite (HAp) composite fiber as a scaffold of ligament regeneration. Chitosan- HAp composite fiber was made by using coagulation method. Chitosan-NaH_2PO_4 solution was coagulated with coagulation bath including calcium ion to get the mono-fiber and then treated with sodium hydroxide solution to form HAp in fiber matrix. The mechanical property of the fiber was improved by the stretching of the wet one because of the orientation of chitosan molecule and the interaction between chitosan and HAp. Maximum stress was improved with increasing of sodium dihydrogen phosphate until 0.03 M. The swelling ratio of the fiber was inhibited by composited with HAp. Additionally, bone-bonding ability was confirmed by SBF soaking tests.

Cover Letter

Dear Professor J. F. Kennedy and M. A. Coimbra
Editor-in-Chief
Carbohydrate Polymers

4 March 2017

Dear Professor J. F. Kennedy and M. A. Coimbra,

Please find enclosed our manuscript entitled “Preparation of chitosan-hydroxyapatite composite mono-fiber using coagulation method and their mechanical properties”, which we would like to submit for publication as a Full Length Article.

In this manuscript, we prepared the chitosan-hydroxyapatite (HAp) composite fibers using coagulation method and revealed their mechanical properties in various stretching speed and various amount of HAp. Chitosan solution contained sodium dihydrogen phosphate was injected in coagulation bath contained calcium hydrochloride. At this step, coagulation of chitosan and forming of amorphous calcium phosphate were carried out. And then the obtained fibers were soaked in sodium hydroxide solution in order to improve chitosan crystalline and transform to HAp from amorphous calcium phosphate. High stretching speed improved crystallinity of chitosan and tensile strength of the fibers. The amount of HAp formation was controlled by the concentration of sodium dihydrogen phosphate in the starting solution. Increasing of concentration of sodium dihydrogen phosphate until 0.03 M in the starting solution improved their tensile properties. The fibers with HAp showed lower swelling ratio and degradation rate than one without HAp. The HAp existed uniformly in chitosan fiber and their shapes were similar to natural bone apatite. Moreover, the HAp growing was observed in simulated body fluid (SBF). The phenomena in this manuscript will be of interest to the readers of *Carbohydrate Polymers*.

We confirm that this manuscript has not been published elsewhere and is not under consideration by another journal. All authors have approved the manuscript and agree with submission to Carbohydrate Polymers. The study was supported by Promotion and Standardization of the Tenure-Track System (Kojinsenbatu)” from Ministry of Education. Culture, Sports, Science and Technology (MEXT), Grants-in-Aid for Challenging Exploratory Research (16K12898) from Japan Society of the Promotion of Science, and the Sasakawa Scientific Research Grant from The Japan Science Society, etc. The authors have no conflicts of interest to declare.

Please address all correspondence to:
Yuki SHIROSAKI
Address: Kyushu Institute of Technology, Hibikino, Wakamatsu-ku, Kitakyushu 808-0196, Japan
Tel&Fax: +81-93-695-6023
E-mail:yukis@lsse.kyutech.ac.jp / yukis@che.kyutech.ac.jp

We look forward to hearing from you at your earliest convenience.
Yours sincerely,

Yuki SHIROSAKI
Kyushu Institute of Technology, Japan

- **This coagulation method was successful to obtain a chitosan-HAp composite fiber.**
- **Stretching improved the orientation and maximum stress of the fibers.**
- **Composition of HAp inhibits swelling and degradation rate of the fibers comparing with chitosan fibers.**
- **The bone-bonding ability was confirmed in chitosan-HAp composite finers.**

Preparation of chitosan-hydroxyapatite composite mono-fiber using coagulation method and their mechanical properties

Takuma Okada[1)], Yuta Nobunaga[2)], Toshiisa Konishi[2)], Tomohiko Yoshioka[2)], Satoshi Hayakawa[2)], Maria Ascensão Lopes[3)], Toshiki Miyazaki[1)], Yuki Shirosaki[4)*]

1) Graduate School of Life Science and Systems Engineering, Kyushu Institute of Technology, 2-4 Hibikino, Wakamatsu-ku, Kitakyushu, Fukuoka 808-0196, Japan

2) Graduate School of Natural Science and Technology, Okayama University, 3-1-1 Tsushima-naka, Kita-ku, Okayama, 700-8530, Japan

3) CEMUC, Departamento de Engenharia Metalúrgica e Materiais, Faculdade de Engenharia, Universidade do Porto, Rua Dr. Roberto Frias, 4200-465 Porto, Portugal

4) Frontier Research Academy for Young Researchers, Kyushu Institute of Technology, 2-4 Hibikino, Wakamatsu-ku, Kitakyushu, Fukuoka 808-0196, Japan

*Corresponding author: yukis@lsse.kyutech.ac.jp

Key word: artificial ligament, fiber, chitosan, hydroxyapatite, coagulation method, mechanical property

Abstract

Autograft has been carried out for anterior cruciate ligament (ACL) reconstruction surgery. However, it has negative aspect because patients lose their healthy ligaments from other part. Sometimes, artificial ligament from synthetic polymer such as PET is used, however it does not have bone-bonding ability and stays long time in body. We focus on a chitosan-hydroxyapatite (HAp) composite fiber as a scaffold of ligament regeneration. Chitosan- HAp composite fiber was made by using coagulation method. Chitosan-NaH_2PO_4 solution was coagulated with coagulation bath including calcium ion to get the mono-fiber and then treated with sodium hydroxide solution to form HAp in fiber matrix. The mechanical property of the fiber was improved by the stretching of the wet one because of the orientation of chitosan molecule and the interaction between chitosan and HAp. Maximum stress was improved with increasing of sodium dihydrogen

phosphate until 0.03 M. The swelling ratio of the fiber was inhibited by composited with HAp. Additionally, bone-bonding ability was confirmed by SBF soaking tests.

1. Introduction

Although autograft is clinically used for reconstructive surgery of anterior cruciate ligament, it has still some problems. For example, it is necessary to extract the ligament tissue from other healthy part of patient's body (Woo *et al*., 1998; Doroski, Brink, & Temenoff, 2007). This method has negative aspect. Although patellar tendon and hamstring are used as a donor site, there are problem of donor site. The donor site has significant clinical abnormalities. Therefor patients need much times for rehabilitation (Kartus, Movin, & Karlsson, 2001). This problem can be solved by using artificial ligament. Artificial ligament got popular from 1980s. Although various artificial ligament was made from carbon fibers, polypropulene, Dacron and polyester, every materials have problems such as cross-infections, immunological response, breakage, debris dispersion, leading to synovitis, chronic effusions, recurrent instability and knee osteoarthritis (Legnani, Ventura, Terzaghi, Borgo, & Albisetti, 2010) There are some successful ACL reconstruction using the artificial ligament, such as PET based material

(Lavoie, Fletcher, & Duval, 2000). It tales shorter time for the rehabilitation using PET fiber than autograft, but there are a lot of the crushed filaments at the joint of the tibial tunnel (Mowbray, McLeod, Barry, Cooke, & O'Brien, 1997) because of PET's bone-non-bonding ability. Our approach is the preparation the new ligament added the bone-bonding ability to PET based one to solve this problem.

We focus on chitosan and hydroxyapatite (HAp) composite fiber. Chitosan is biodegradable polymer (Chandy & Sharma, 1990; Jayakumar, Pradaharan, & Muzzarelli, 2011) and HAp is fundamental inorganic component for exhibiting bone-bonding ability (Davidenko, Carrodeguas, Peniche, Solís, & Cameron, 2010; Tuzlakoglu & Reis, 2007; Manjubala, Ponomarev, Wilke, & Jandt, 2008). The chitosan-HAp fiber can be prepared by coagulation system using calcium chloride solution (Tamura *et al*., 2004). This method is suitable for biomaterial fabrication because of synthesis with low toxicity materials. However, the obtained fiber did not have sufficient mechanical strength for artificial ligament, since excessive calcium ion decreased crystallinity of chitosan. Yamaguchi *et al.*, focused on crystallinity of chitosan and obtained chitosan fibers from tendon of clubs by deacetylation. The obtained chitosan fiber has good crystallinity

because chitin of club tendon has good crystallinity (Yamaguchi *et al*., 2003). However use of row material is difficult to control the length and shape of the obtained fibers. They also modified HAp on the fibers to get the core-shell type composite fibers. The core-shell type composite fibers have interface clearly between chitosan and HAp and the shear stress becomes higher at the interface to induce the clacks. On the other hand, the fiber is exfoliated from natural bone because HAp exists only surface of fibers after the degradation of chitosan. In this study, we prepared chitosan-HAp composite fiber which is dispersed HAp inside the chitosan matrix with coagulation method. The mechanical property, the biodegradability, and the bone-bonding ability were examined.

2. Materials and Methods

2.1. Preparation of chitosan-HAp composite fibers

The chitosan powder (Medium molecular weight, Sigma-Aldrich®, St. Louis, USA) and sodium dihydrogen phosphate (NaH_2PO_4 Nacalai Tesque Inc., Kyoto, Japan) was dissolved in 0.1 M aqueous acetic acid to obtain 3.5 wt% chitosan and 0 (P0), 0.01 (P1), 0.02 (P2), 0.03 (P3) and 0.04 (P4) M NaH_2PO_4 by planetary centrifuged mixer (ARE-310, Thinky, Tokyo, Japan). Coagulation bath was prepared by mixing saturated calcium

chloride ($CaCl_2$ Nacalai Tesque Inc., Kyoto, Japan) aqueous solution and ethanol (Wako Pure Chemical Industries, Ltd., Osaka, Japan) at 1:1 volume ratio. The chitosan-NaH_2PO_4 solution was injected in the coagulation bath from nozzle of syringe with 0.5 mm hole by 1 mL/min and rolled up with less than 1 rpm by roller to get the wet fiber. The obtained wet fiber was soaked in 100% ethanol for 5 minutes and then soaked in 0.2 M sodium hydroxide aqueous solution for 30 minutes to remove the exceeded acetic-acid. The fiber was washed with distilled water to remove the exceeded sodium hydroxide aqueous solution. The fiber was stretched with two rollers which rolling speed 2:3 (10/20, 20/30, 30/45 rpm). Finally, the fiber was dried at room temperature under the desiccator.

2.2 Characterization of the fiber structure

In order to confirm crystallinity of chitosan and formation of HAp, the obtained fiber was examined by X-ray diffraction (TF-XRD; MXP3V, Mac Science, Co., Yokohama, Japan) with the angle of the X-ray (CuKα) was fixed at $\theta = 1°$ and the detector was step-scanned around the 2θ axis from 20° to 40° at a rate of 0.02°/step with a count time of 2 seconds. The orientation of the fiber was observed by inverted microscope (IX73, Olympus Co.,

Tokyo, Japan) under crossed-Nicols. The surface morphology was observed by scanning electron microscope (SEM) (JMS-6010 PLUS/LA, JEOL, Tokyo, Japan) with energy dispersive X-ray microanalyzer (EDX). Before observation, the fibers were coated with Pt/Pd which thickness was around 20 nm (MSP-1S Magnetron Sputter, Vacuum Device Inc., Mito, Japan). The nanostructure of the fiber was observed by Transmission Microscope (TEM) (JEM-2100, JEOL, Tokyo, Japan). The fibers were put into epoxy resin. TEM samples with around 65 nm thickness were prepared by using ultra microtome (Leica EM UC6, Leica, Wetzlar, Germany). After that, the samples were put on Hi-Res carbon coated copper grid mesh (HRC-C10, Okenshoji Co., Ltd., Tokyo, Japan). Thermogravimetry (TG) and differential thermal analysis (DTA) were examined by Thermal Analysis System (2000S, Mac Science Co., Yokohama, Japan) in the temperature range from room temperature to 900°C with a heating rate of 10°C/min. From the result of TG, the inorganic/organic ratio in the composite fibers was calculated.

2.3. Mechanical property of the composite fibers

Mechanical properties of the fibers were measured by creep meter (RE2-3305C,

YAMADEN Co., Ltd., Tokyo, Japan). The sample fibers with 10 mm were sandwiched both side with paper and adhesion reagent (Fig. 1). Tensile test was carried out at 0.5 mm/sec.

2.4. Swelling behavior and enzymatic degradability

The obtained fiber was soaked in phosphate buffer saline (PBS pH = 7.4) for 1 hour at 37°C. Swelling ratio of the fibers was estimated from weight change (Eq. 1). The swollen fibers also are measured their mechanical properties after soaked for 1 h. There biodegradability was evaluated from weight change (Eq. 2) after soaked in 2.5 μg/mL lysozyme solution at 37°C up to 9 weeks. The concentration of lysozyme is followed the concentration of human blood plasma (Brouwer, van Leeuwen-Herberts, & Otting-van de Ruit, 1984). Swelling ration and weigh loss were calculated by equation (1) and (2), respectively.

$$\text{Swelling ratio} / \% = (|W_{\text{Swelled}} - W_{\text{initial}}| / W_{\text{initial}}) \times 100 \quad \text{Eq.(1)}$$

$$\text{Weight loss} / \% = (|W_{\text{soaked}} - W_{\text{initial}}| / W_{\text{initial}}) \times 100 \quad \text{Eq.(2)}$$

2.5. Evaluation of bone bonding ability of the composite fibers

Bone bonding ability was tested by apatite formation in SBF (Kokubo & Takadama,

2006) at 37°C for 8 days. After soaked, the samples were characterized by XRD and SEM.

3. Results

3.1. Structural characterization

This coagulation method was successfully to get the fibers. The diameter of P0 to P4 were 194±3, 214±10, 225±13, 228±8, 269±14 μm, respectively. After chitosan solution was injected into the coagulation bath including calcium ions, the color of chitosan solution gradually turned white from light yellow. The fiber shape was remained at all steps after coagulation. XRD patterns at each preparation step are shown in Fig. 2. The fiber of after coagulation, chitosan peak around $2\theta = 20^{o}$ was disappeared as shown in Fig. 2 (b). After sodium hydroxide treatment, this peak and new peak assigned to HAp were detected again as shown in Fig. 2 (c). From Fig. 3, the peaks assigned to HAp increased with the concentration of sodium dihydrogen phosphate (P0-P4). The inorganic/organic ratio was estimated from TG-DTA is shown in Fig. 4. The inorganic/organic ratio got linear increasing as the concentration of sodium dihydrogen phosphate increased. The images of the fibers were observed by inverted

microscope under crossed-Nicols as shown in Fig. 5. Comparing P0 (Fig.(a), (b)) to P2 (Fig.(c), (d)), P0 is darker than P2. SEM images of P2 and the results of EDX analysis are shown in Fig. 6. From SEM images (×1000), HAp particles were not observed. However, EDX analysis showed that phosphorus and calcium atoms were existed inside of fiber. TEM images of P2 is shown in Fig. 7. HAp particles are 20.5 ± 6.1 nm at cross-section and 50.7 ± 9.7 nm at longitudinal-section.

3.2. Mechanical property

The results of tensile test of the fibers with different stretching speed are shown in Fig. 8. The tensile strength was gradually high with increasing of stretching speed. When stretching speed was more than V1 / V2 = 30 / 45 (rpm), the fiber was broken. The maximum stress of V1 / V2 = 10 / 15, 20 / 30 and 30 / 45 (rpm) were 48.3±7.4, 93.5±16.4 and 112.9±22.2 MPa. The maximum strain of V1 / V2 = 10 / 15, 20 / 30 and 30 / 45 (rpm) were 7.03±4.6, 12.5±5.2 and 9.30±4.7 %. The tensile properties of fibers (P0-P4) with V1 / V2 = 30 / 45 (rpm) at dry state is shown in Fig. 9. The maximum strength of P0, P1, P2, P3 and P4 were 103.9±29.5, 110.9±18.6, 113.3±22.4, 137.2±31.8 and 61.5±4.17 MPa, respectively.

3.3. *Swelling behavior and enzymatic degradability*

The swelling ratio is shown in Fig. 10. The swelling ratio of all fiber was saturated after 30 minutes in PBS and the fibers with HAp is lower than without HAp. The tensile property of the swelled fibers soaked for 1h is shown in Fig. 11. The maximum strength of P0, P1, P2 and P3 were 14.0±1.6, 9.9±0.9, 25.0±2.4 and 24.0±7.0 MPa, respectively. The maximum strain of P0, P1, P2 and P3 were 119.0±18.0, 50.2±8.5, 41.2±5.1, 52.0±6.5 MPa, respectively. Comparing with dry state, maximum stress was dramatically decreased in all samples and the strain ratio was increased in all samples. Regarding biodegradation test shown in Fig. 12, the weight loss was similar behavior until 6 weeks. However, weight loss of the fibers with HAp (P1, P2 and P3) were mildly comparing the fibers without HAp (P0).

3.4. Evaluation of bone bonding ability

XRD patterns of the P0 and P2 of before and after soaking in SBF are shown in Fig. 13. The peak of HAp was not confirmed at P0 before and after soaking in SBF. On the other hand, the peak of HAp at P2 had little increased after soaking SBF compering to before soaking. SEM images of the fibers (P0 and P2) before and after soaking in SBF were

shown in Fig. 14. Particle was not confirmed in P0 before and after soaking. However, the surface of P2 after soaking was observed spherical particles.

4. Discussion

Chitosan molecules have inter-molecular hydrogen bond between O6-N2 (Okuyama, Noguchi, Miyazawa, Yui, & Ogawa, 1997), but the amino group of chitosan is protonated in the acetic acid solution. According to Fig. 2, the crytallinity of chitosan was lost after soaking in coagulation bath including calcium ion and then improved with HAp formation after sodium hydroxide aqueous solution treatment. These results insist that inter-molecular hydrogen bonds among chitosan molecules were broken after coagulation because the coordinated bonds were formed between calcium atoms and amino groups of chitosan. Calcium phosphate precipitates with appropriate calcium and phosphate ions formed HAp crystal at pH value greater than 6.8 (Brown, Patel, & Chow, 1975). According to Fig. 4, the inorganic/organic ratio increased linearly as the concentration of sodium dihydrogen phosphate in the initial chitosan solution. It means that the amounts of HAp depend on the concentration of sodium dihydrogen phosphate in chitosan solution. In this study, it is concluded that amorphous calcium phosphate

formed in the coagulation bath including calcium ion and then amorphous calcium phosphate transformed to HAp in sodium hydroxide solution. Although HAp particles were not observed under SEM, EDX analysis showed existing of calcium and phosphor atom uniformly on the surface and inside of fibers. Moreover, HAp particles with the diameter 20.5 ± 6.1 nm in cross-section and 50.7 ± 9.7 nm longitudinal-section were calculated from TEM images. These results shows that HAp composites with chitosan in nanoscale and dispersed inside of fibers without phase separation. The particle size of HAp in natural bone is 20 and 50 nm (Hench & Jones, 2005). Because the HAp particle in this fiber is similar to HAp in natural bone at the point of its shape, it is expected that this fiber can bond with natural bone *in vivo*.

Fig. 8 shows that maximum stress enhanced with increasing of stretching speed. And Fig. 4 shows that stretching improved the orientation of chitosan. These results mean that improving chitosan orientation enhanced maximum stress of fibers. Increasing of the concentration of sodium dihydrogen phosphate in the chitosan solution enhanced fibers until 0.03 M (P3), however, maximum stress and strain was lowest at 0.04 M (P4). Moreover, Fig. 3 shows the amount of HAp depends on the amount of the amount of

sodium dihydrogen phosphate. These results insist that the interaction between HAp and chitosan enhances the maximum stress however in the case of concentration of sodium dihydrogen phosphate was more than 0.04 M, the fiber got too harder because the increase of HAp amount.

At wet state tensile tests, maximum stress decreased at all fibers and strain increased (Fig. 11). The maximum stresses of P3 and P2 were higher than P1 and P0. The behavior of P0 was completely deferent from other fibers. The swelling ratio of the P0 was about 3 however P3, P2, and P1 were about 2. These results insist that chitosan fibers composite with HAp has interaction between HAp and chitosan and prevents swelling compering with just chitosan fibers. Therefore, maximum stress of P2 and P3 was stronger than P0 in wet state. It is expected that chitosan form the coordinate bond with HAp, which is stronger than the inter-molecular hydrogen bond between the chitosan molecules.

Conclusion

This coagulation method was successful to obtain a chitosan-HAp composite fiber. Stretching improved the orientation and maximum stress of the fibers. The amount of

HAp depends on the concentration of sodium dihydrogen phosphate in chitosan-NaH_2PO_4 solution. Increasing the concentration of sodium dihydrogen phosphate in chitosan-NaH_2PO_4 solution until 0.03 M improved maximum stress of the fibers. Composition of HAp inhibits swelling of the fibers comparing with chitosan fibers. The bone-bonding ability was confirmed in chitosan-HAp composite finer because the shape of HAp was similar to HAp in natural bone and grew in SBF.

Acknowledgement

A part of this work was supported by "Promotion and Standardization of the Tenure-Track System (Kojinsenbatu)" from Ministry of Education. Culture, Sports, Science and Technology (MEXT), Japan, Grants-in-Aid for Challenging Exploratory Research (16K12898) from Japan Society of the Promotion of Science, Sasakawa Scientific Research Grant from The Japan Science Society, NIMS microstructural characterization platform (NMCP) as a program of "Nanotechnology Platform" of MEXT, and Portuguese Foundation for Science and Technology (FCT: UID/EMS/00285/2013). We are grateful Ms. I. Koda in NMCP for preparing TEM samples.

References

Brouwer, J., van Leeuwen-Herberts, T., Otting-van de Ruit, M. (1984). Determination of lysozyme in serum, urine, cerebrospinal fluid and feces by enzyme immunoassay. *Clinica Chimica Acta; International Journal of Clinical Chemistry*, 142, 21-30.

Brown, W. E., Patel, P. R., Chow, L. C. (1975). Formation of $CaHPO_4 \cdot 2H_2O$ from enamel mineral and its relationship to caries mechanism. *Journal of Dental Research*, 54, 475-481.

Chandy, T., Sharma, C. P. (1990). Chitosan-as a biomaterial. *Biomaterials Artificial Cells and Artificial Organs*, 18, 1-24.

Davidenko, N., Carrodeguas, R. G., Peniche, C., Solís, Y., Cameron, R. E. (2010). Chitosan/apatite composite beads prepared by in situ generation of apatite or Si-apatite nanocrystals. *Acta Biomaterialia*, 6, 466-476.

Doroski, D. M., Brink, K. S., Temenoff, J. S. (2007). Techniques for biological characterization of tissue-engineered tendon and ligament. *Biomaterials*, 28, 187-202.

Hench, L., Jones, J. (2005) *Biomaterials, Artificial Organs and Tissue Engineering*, Cambridge: Woodhead.

Jayakumar, R., Pradaharan, M., Muzzarelli, R. A. A. (2011). *Chitosan for Biomaterials II*. Advanced in Polymer Science 244, New York: Springer.

Kartus, J., Movin, T., Karlsson, J. (2001). Donor-site morbidity and anterior knee problems after anterior cruciate ligament reconstruction using autografts. *The Journal of Arthroscopic & Related Surgery*, 17, 971-980.

Kokubo, T., Takadama, H. (2006). How useful is SBF in predicting in vivo bone bioactivity?, *Biomaterials*, 27, 2907-2915.

Lavoie, P., Fletcher, J., Duval, N. (2000). Patients satisfaction needs as related to knee stability and objective findings after ACL reconstruction using the LARS artificial ligament. *The Knee*, 7, 157–163.

Legnani, C., Ventura, A., Terzaghi, C., Borgo, E., Albisetti, W. (2010). Anterior cruciate ligament reconstruction with synthetic grafts. A review of literature. *International Orthopaedics*, 34, 465-471.

Manjubala, I., Ponomarev, I., Wilke, I., Jandt, K. D. (2008). Growth of osteoblast-like cells on biomimetic apatite-coated chitosan scaffolds. *Journal of Biomedical Materials Research Part B: Applied Biomaterials*, 84B, 7-16.

Mowbray, M. A. S., McLeod, A. R. M., Barry, M., Cooke, W.D., O'Brien, T.K. (1997). Early failure in an artificial anterior cruciate ligament scaffold. *The Knee*, 4, 35–40.

Okuyama, K., Noguchi, K., Miyazawa, T., Yui, T., Ogawa, K. (1997). Molecular and Crystal Structure of Hydrated Chitosan. *Macromolecules*, 30, 5849-5855.

Tuzlakoglu, K., Reis, R. L. (2007). Formation of bone-like apatite layer on chitosan fiber mesh scaffolds by a biomimetic spraying process. *Journal of Materials Science*, 18, 1279-1286.

Tamura, H., Tsuruta, Y., Itoyama, K., Worakitkanchanakul, W., Rujiravanit, R., Tokura, S. (2004). Preparation of chitosan filament applying new coagulation system. *Carbohydrate Polymers*, 56, 205-211.

Woo, S. L-Y., Fox, R. J., Sakane, M., Livesay, G. A., Rudy, T. W., Fu, F. H. (1998). Biomechanics of the ACL, Measurements of in situ force in the ACL and knee kinematics. *The Knee*, 5, 267-288.

Yamaguchi, I., Itoh, S., Suzukie, M., Sakane, M., Osaka, A., Tanaka, J. (2003). The chitosan prepared from crab tendon II The chitosan / apatite composites and their application to nerve regeneration. *Biomaterials*, 24, 2031-2036.

Figure Captions

Fig. 1 An illustration of the sample for the tensile test.

Fig. 2 XRD patterns of the P2 fibers at each preparation step. (a) Dried chitosan solution, (b) after coagulation, (c) after sodium hydroxide solution treatment, and (d) after stretched.

Fig. 3 XRD patterns of the fibers with different concentration of sodium dihydrogen phosphate.

Fig. 4 Inorganic / organic ratio calculated from TG-DTA data of the fibers with different concentration of sodium dihydrogen phosphate.

Fig. 5 Images of the P2 fiber by microscope with crossed-Nicols at each step, (a) dried before stretching and (b) its rotated 45° position, (c) after stretching and (d) its rotated 45° position. Arrows show the direction of nicols.

Fig. 6 SEM images and EDX analysis of the P2 fiber surface and cross-section.

Fig. 7 TEM images of the P2 fiber cross-section and longitudinal-section.

Fig. 8 Stress-strain curves of the P2 fiber with different stretching speed, V1 / V2 (rpm) = 10 / 15 (a), 20 / 30 (b), and 30 / 45 (c).

Fig. 9 Stress-strain curves of t the fibers with different concentration of sodium dihydrogen phosphate at V1 / V2 = 30 / 45 (rpm).

Fig. 10 Swelling ratio of the fibers with different concentration of sodium dihydrogen phosphate until 1 hour.

Fig. 11 Stress-strain curves of the fibers with different concentration of sodium dihydrogen phosphate at V1 / V2 = 30 / 45 (rpm) under wet condition.

Fig. 12 Weight loss of the fibers with different concentration of sodium dihydrogen phosphate until 9 weeks.

Fig. 13 XRD patterns of the P0 and P2 fibersbefore and after soaking in SBF. (a) and (b) are P0 before and after soaking in SBF, (c) and (d) are P2 before and after soaking in SBF.

Fig. 14 SEM images of P2 fiber surface before and after soaking for 8 days in SBF. (a) and (b) are before and after soaking in SBF.

Figure1

Click here to download high resolution image

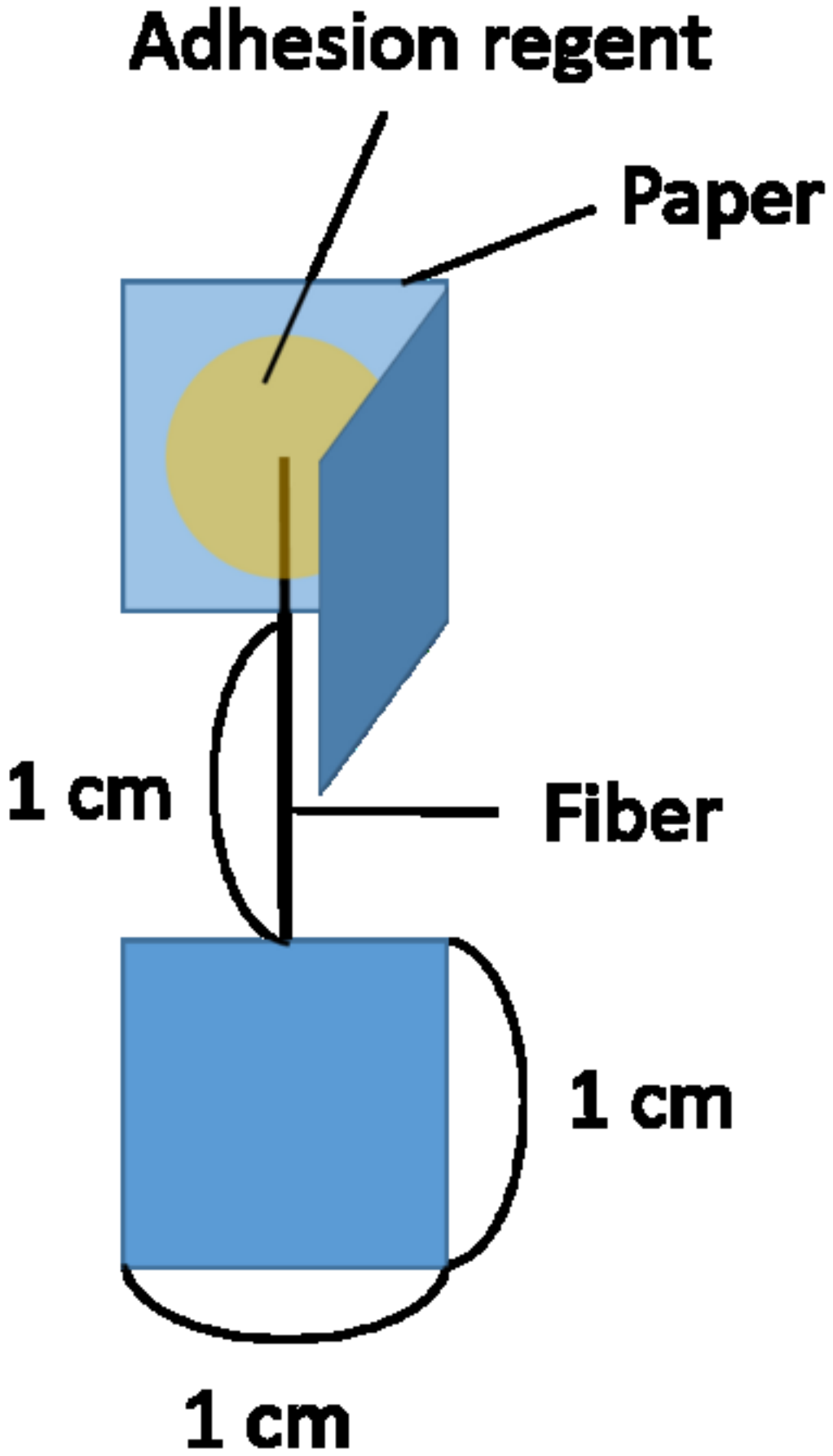

Figure2

Click here to download high resolution image

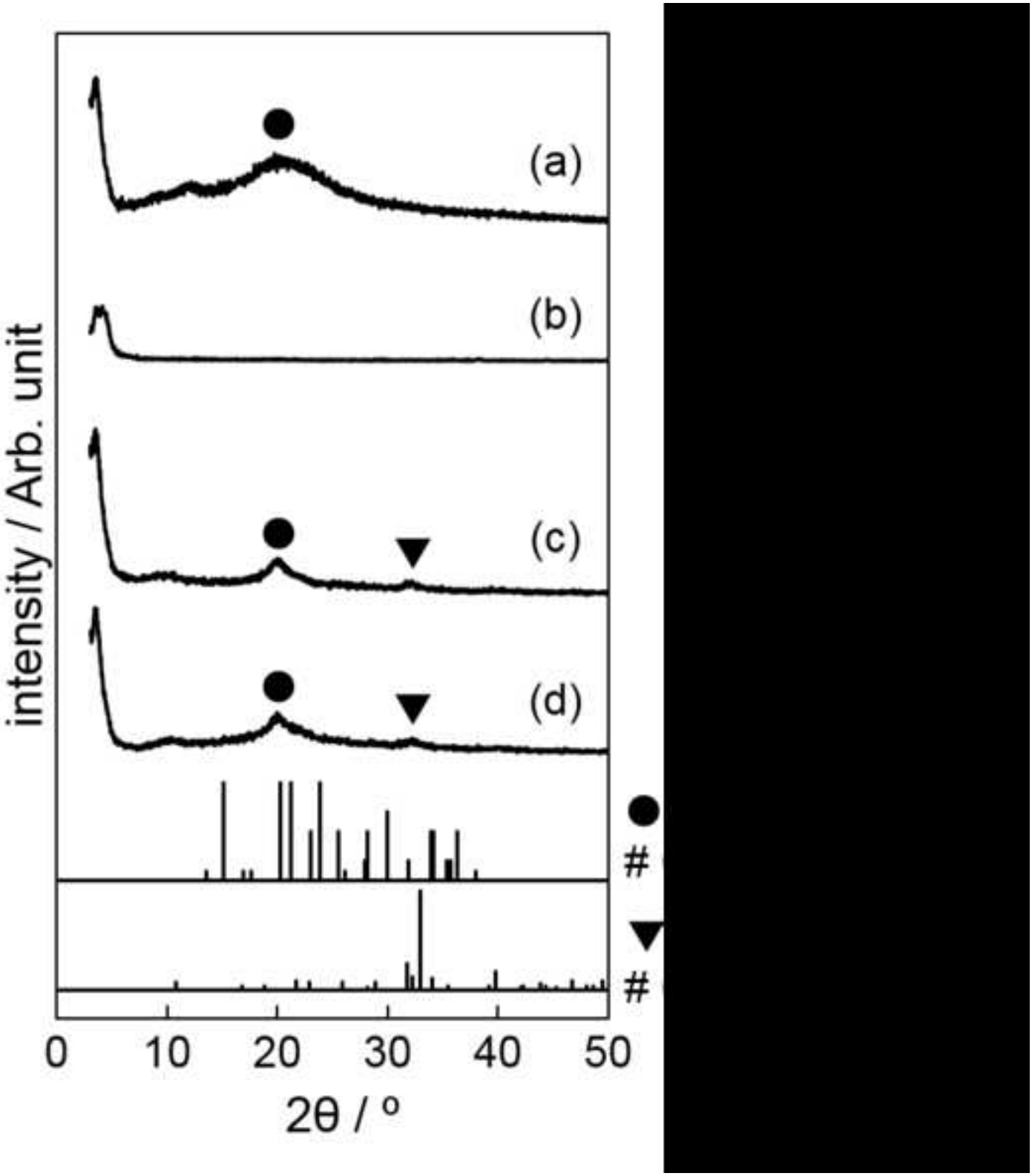

Figure3

Click here to download high resolution image

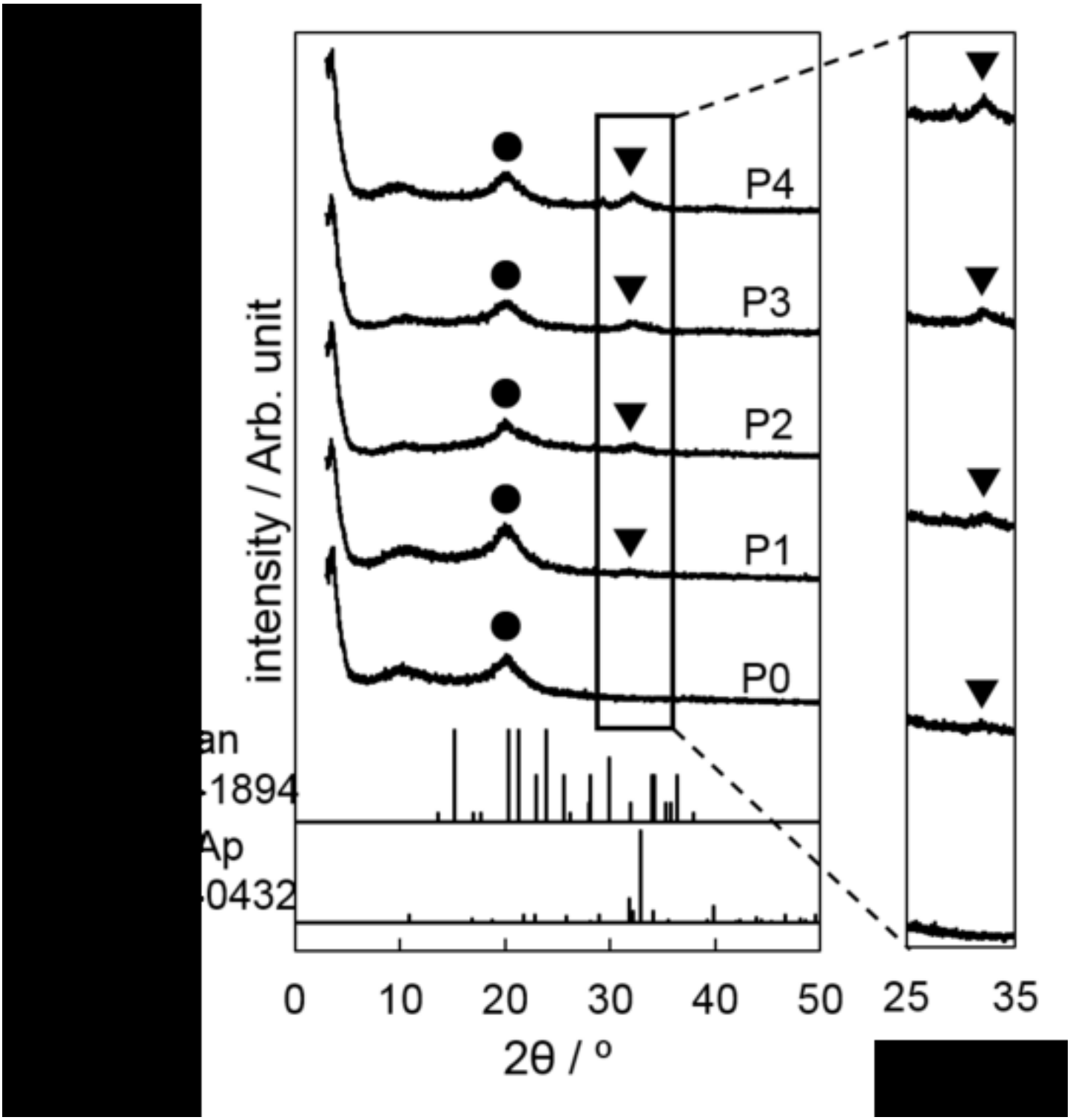

Figure4

Click here to download high resolution image

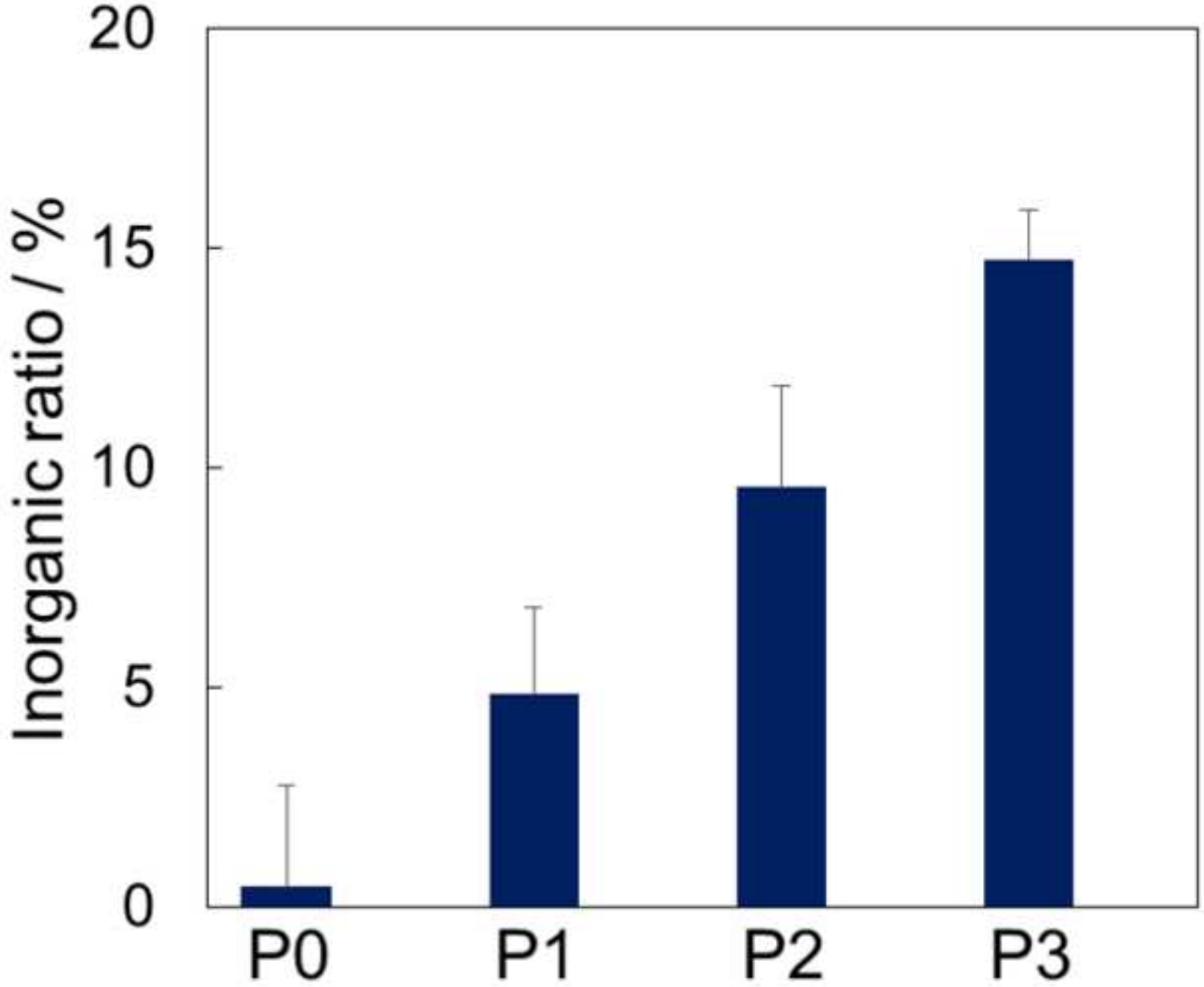

Figure5
Click here to download high resolution image

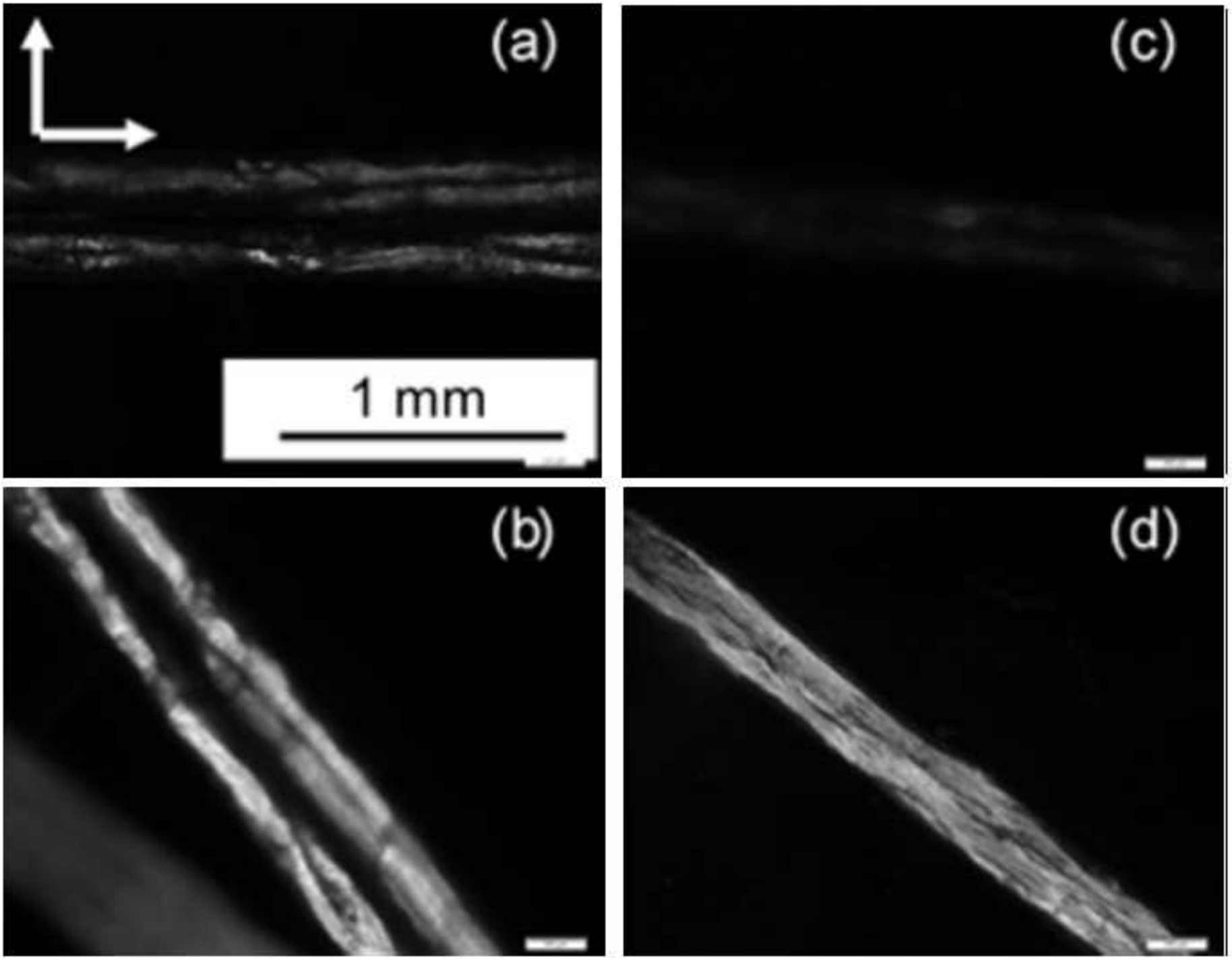

Figure6

Click here to download high resolution image

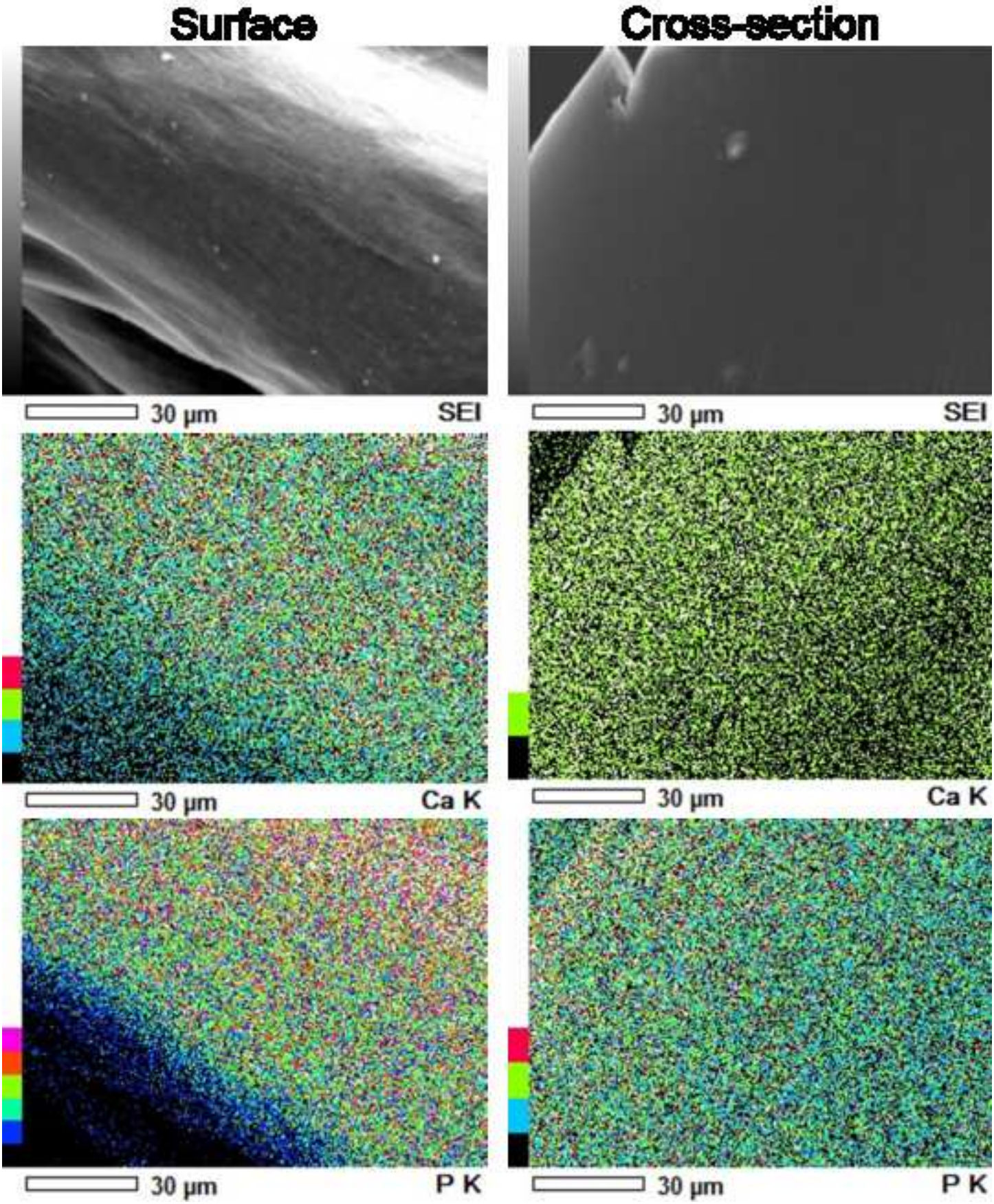

Figure7

Click here to download high resolution image

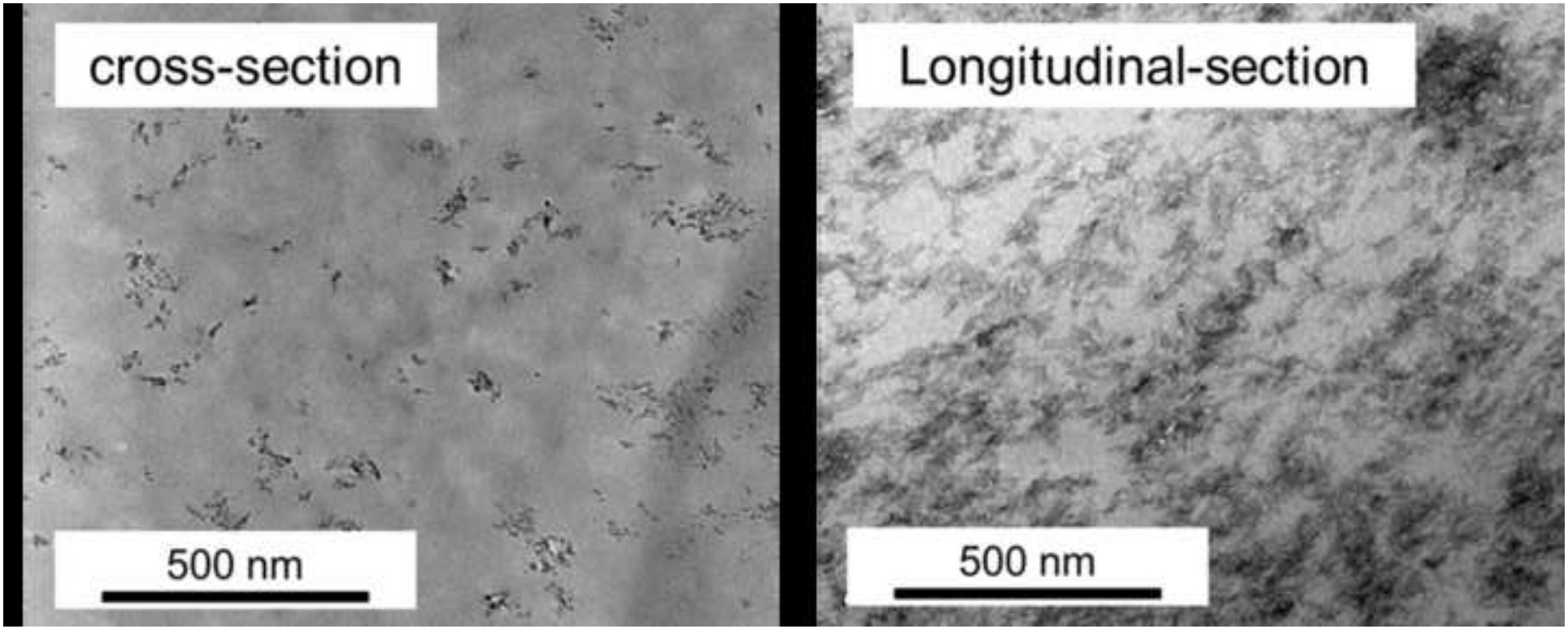

Figure8
Click here to download high resolution image

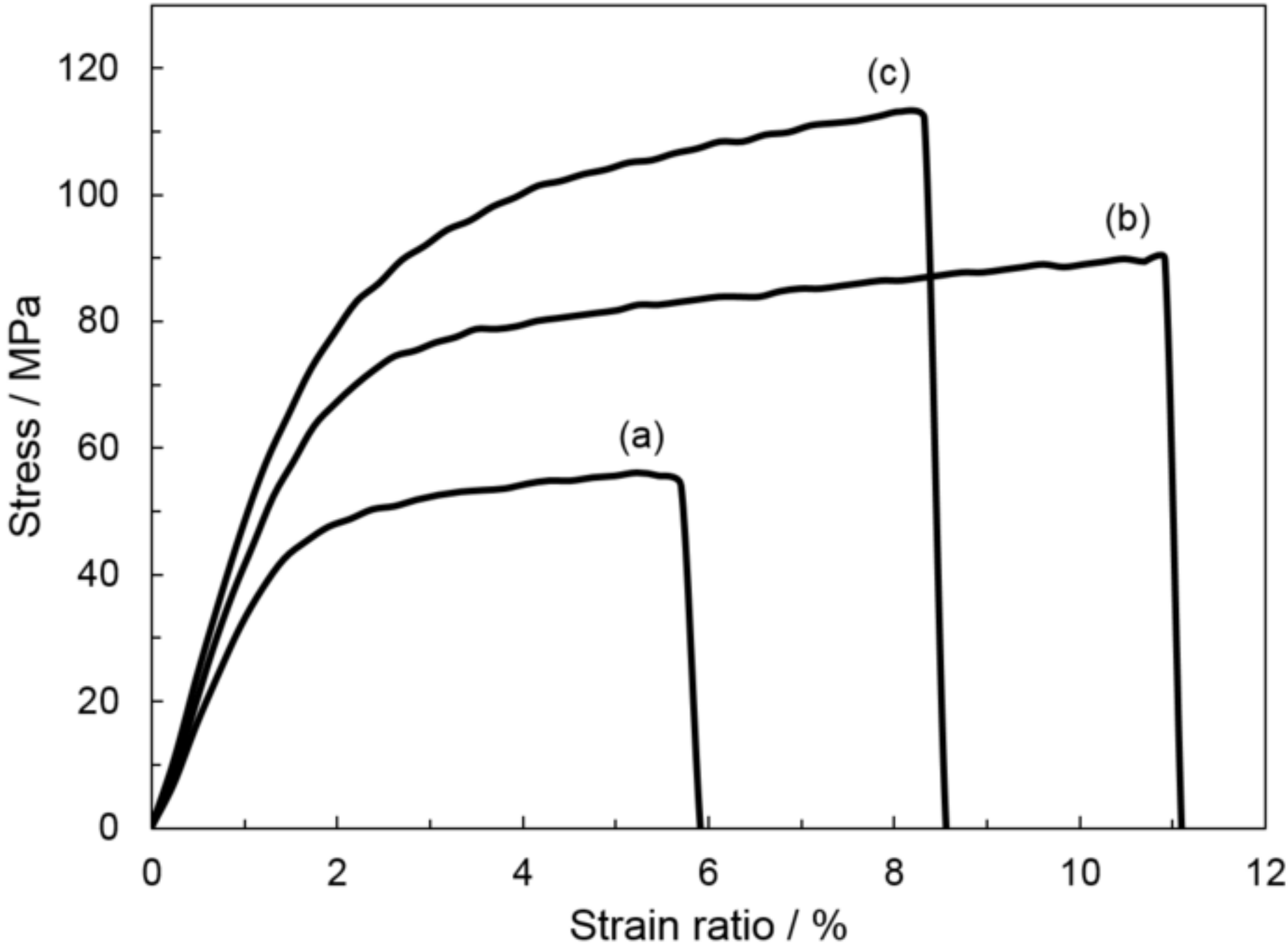

Figure9

Click here to download high resolution image

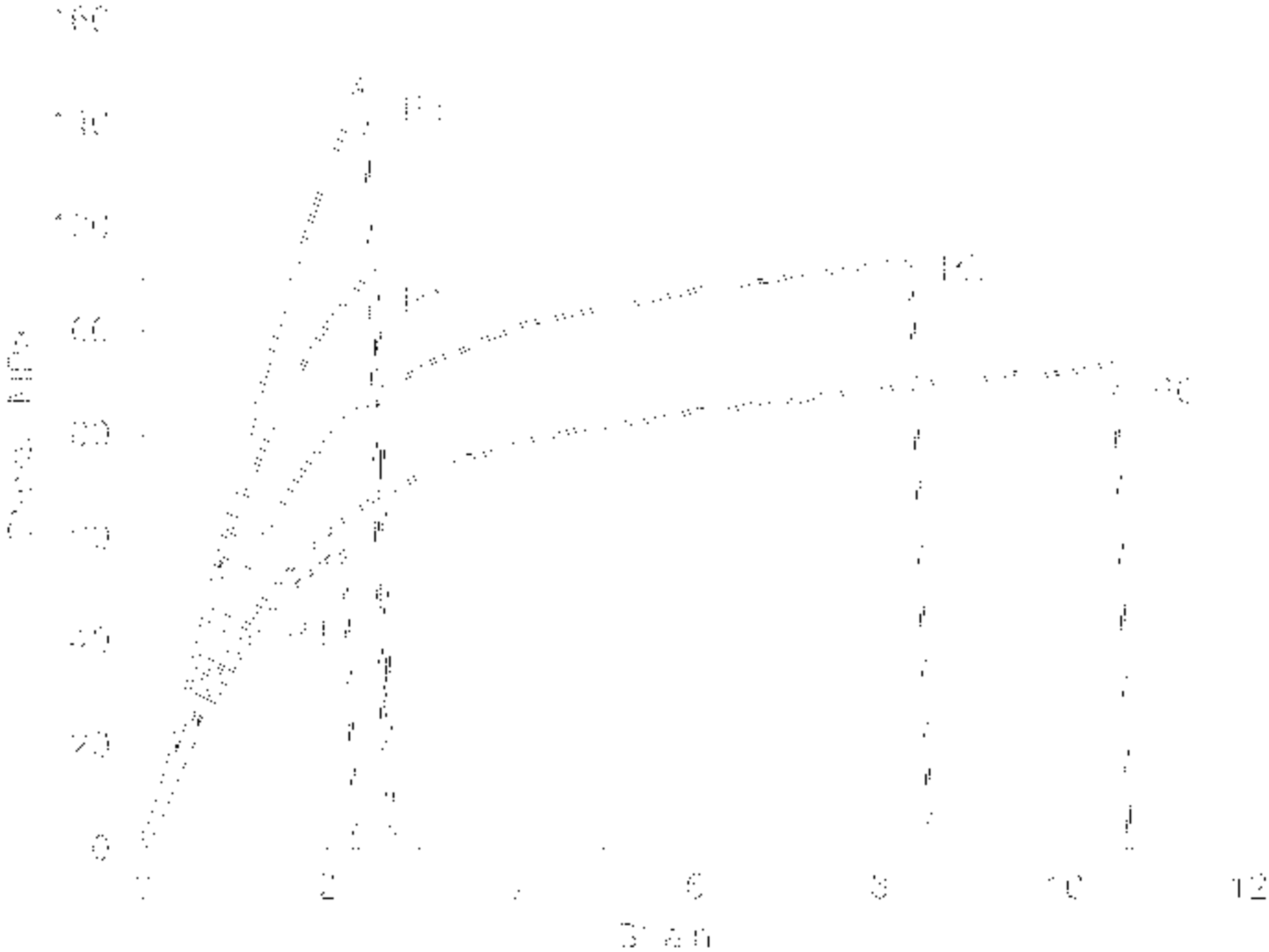

Figure10

Click here to download high resolution image

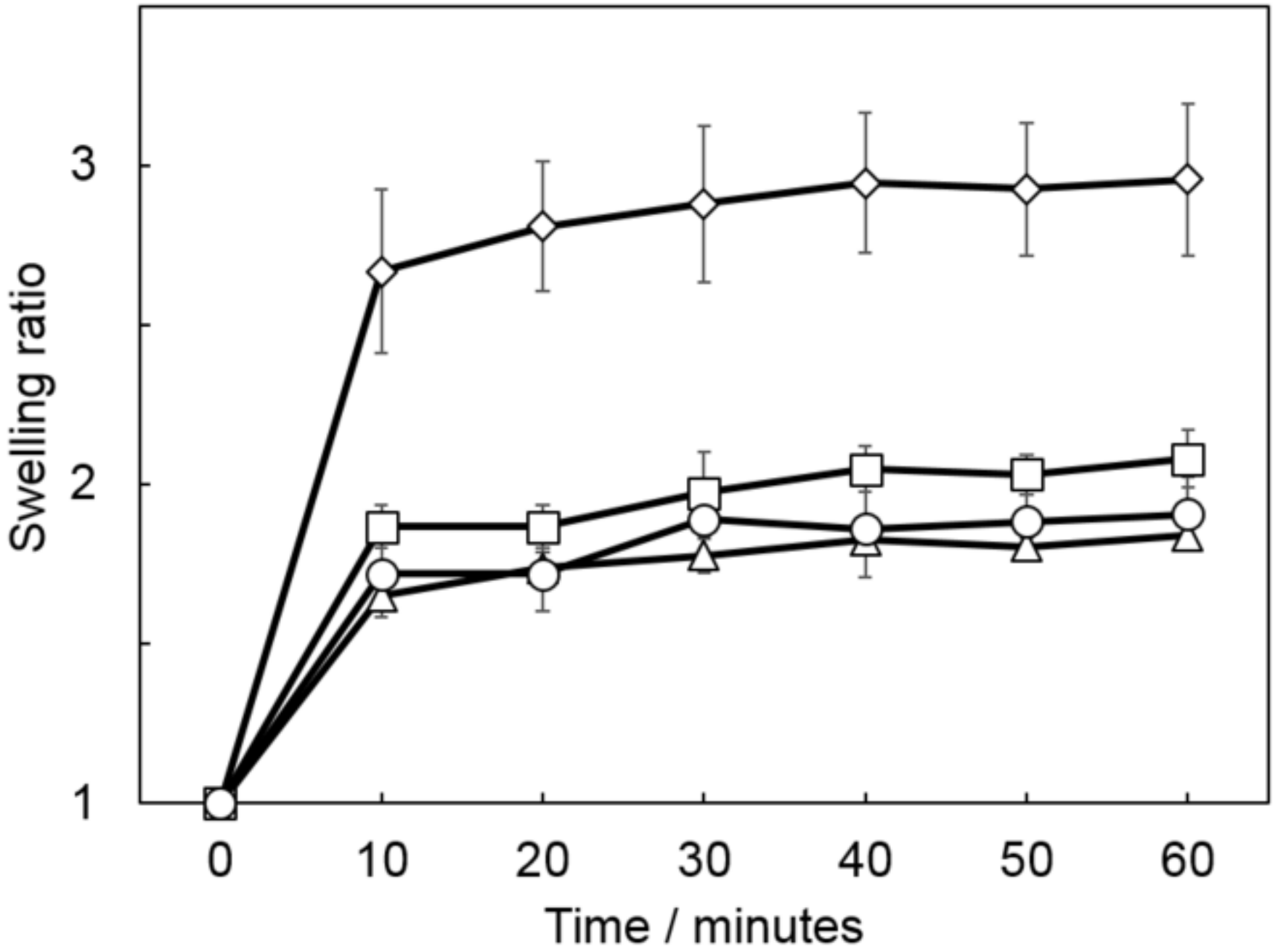

Figure11

Click here to download high resolution image

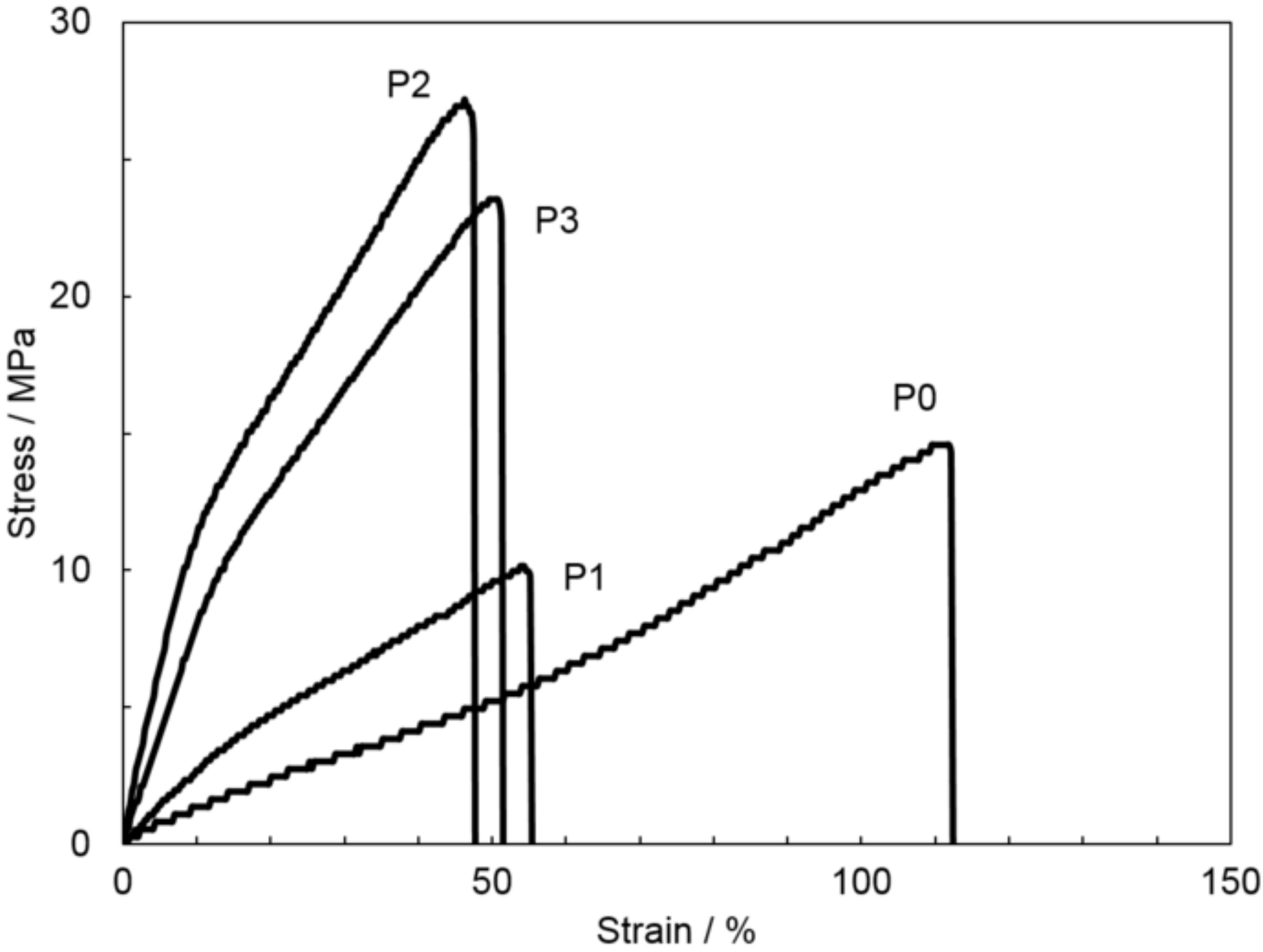

Figure12

Click here to download high resolution image

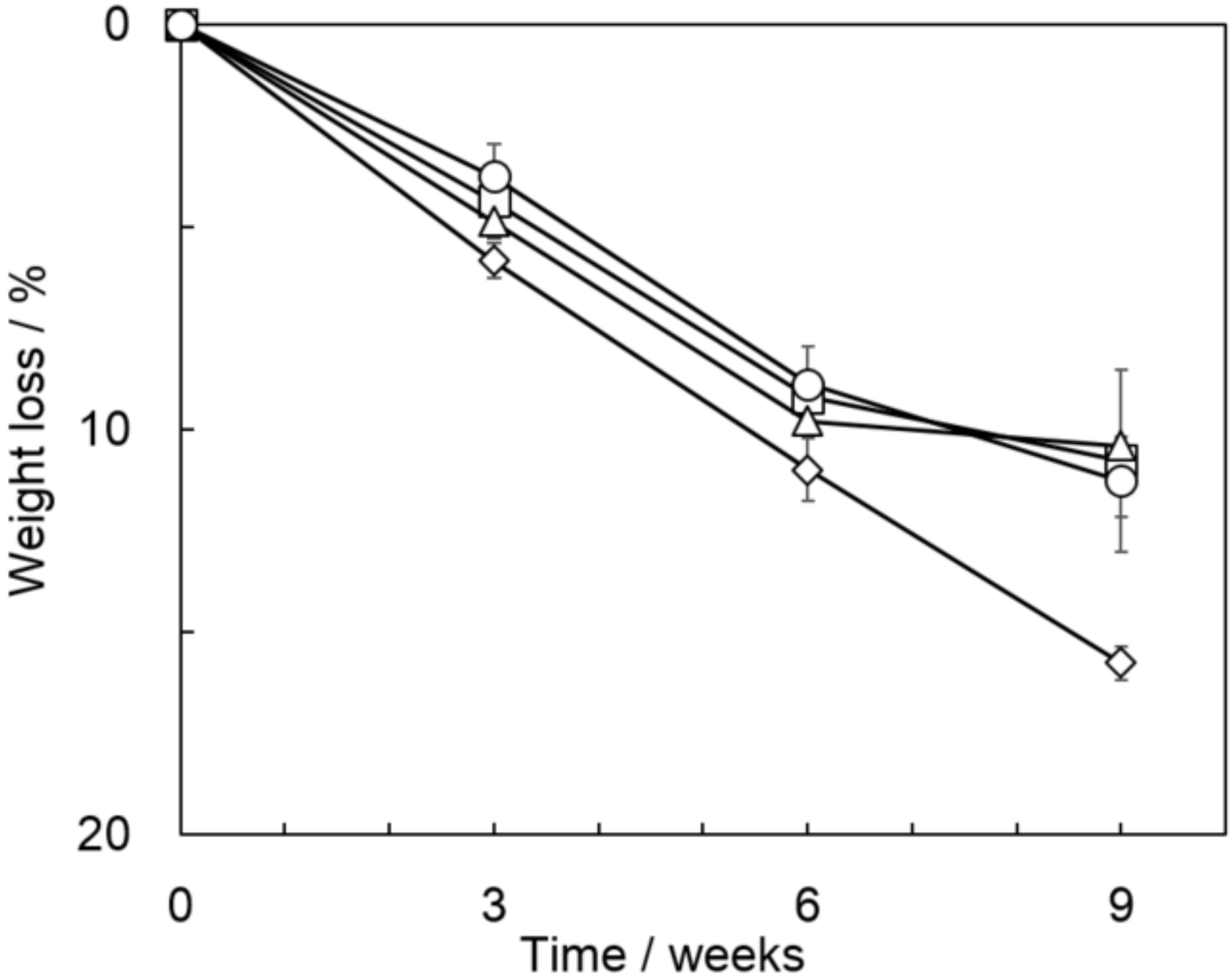

Figure13

Click here to download high resolution image

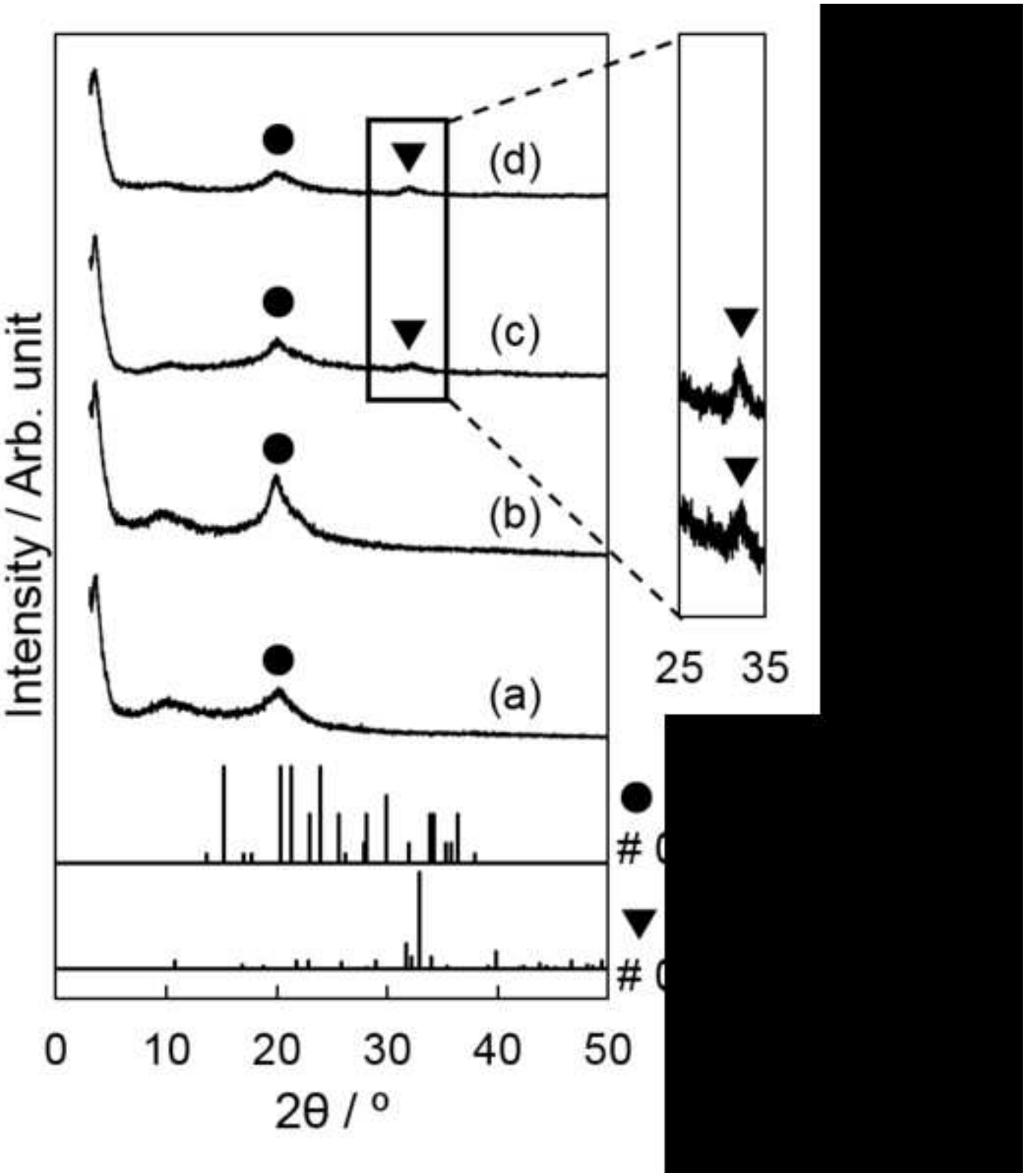

Figure14

Click here to download high resolution image